

Technical Note 802: Photothermal Characteristics of Gold Nanorods

Gold nanorods (GNRs) exhibit transverse and longitudinal surface plasmon resonances that correspond to electron oscillations perpendicular and parallel to the rod length direction, respectively. Their longitudinal surface plasmon wavelengths (LSPWs) are tunable from the visible to infrared regions. Their absorption cross sections are at least five orders larger than those of conventional dyes, and the light scattering by Au nanorods is several orders larger than the light emission from strongly fluorescent dyes.¹⁻³ The tunability in the LSPW, together with strongly enhanced scattering and absorption at the LSPW, makes GNRs useful for the formation of many functional composite materials, for example, with hydrogel,^{4,5} polymers,^{6,7} silica,⁸ and bacteria.⁹ GNRs also have an axial surface plasmon resonance (SSPR), though one-third that of the LSPR, is still many orders of magnitude greater than quantum dots and nanoshells. GNRs also offer advantages of good biocompatibility, facile preparation, and conjugation with a variety of biomolecular ligands, antibodies, and other targeting moieties.¹⁰ They have therefore found wide applications in biochemical sensing,¹¹ biological imaging, medical diagnostics, and therapeutics.¹²⁻¹⁶ Further, GNRs have found application in materials and optics, including polarizers, filters, and to improve the storage density in compact disks.

The effectiveness of GNRs as scattering-based biomedical imaging contrast agents and as photothermal therapeutic agents is strongly dependent on their scattering and absorption cross sections. In general, high scattering cross sections are favorable for cellular and biological imaging based on dark-field microscopy, while large absorption cross sections with small scattering losses allow for photothermal therapy with a minimal laser dosage. In addition, the LSPWs of GNRs are strongly desired to be in the spectral range of 650–900 nm (refer to Figure 1). Light irradiation in this region can penetrate deeper in tissues and cause less photodamage than UV–visible irradiation.¹⁷ Therefore, the ability to tailor both scattering and

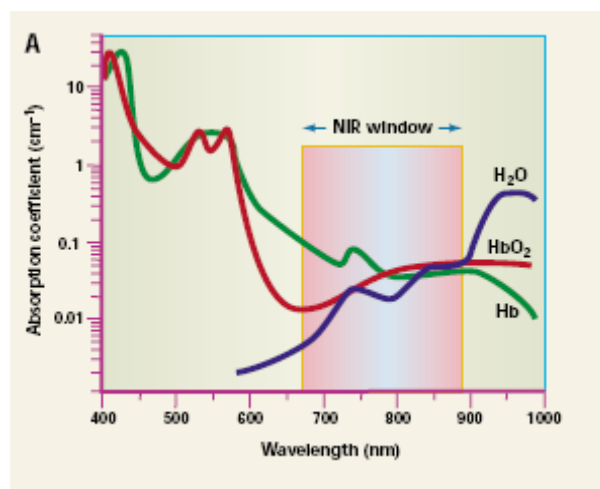


Figure 1. The NIR window is ideally suited for *in vivo* imaging because of minimal light absorption by hemoglobin (<650 nm) and water (>900 nm). From Zauner, W.; et al. *J. Control. Rel.* 2001, 71, 39.

absorption of GNRs with different LSPWs is of ultimate importance for practical *in vivo* biomedical imaging and therapeutic applications.¹⁸⁻²⁰

In order to better characterize the photothermal efficiencies of GNRs, since both absorption and scattering make up the extinction value we measure by UV-VIS, we need to determine the percentage that each contributes. These values are highly dependent on the axial diameter of the GNRs. From Ni et al.,²¹ the scattering/extinction ratio as a function of axial diameter is given in Fig. 2. From this

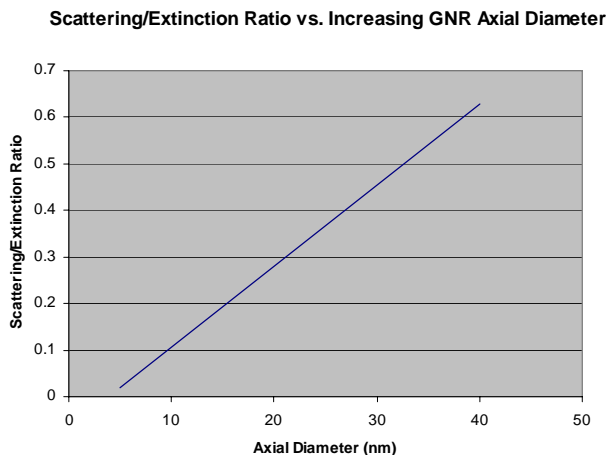


Figure 2 Scattering/Extinction Ratio vs. GNR Axial Diameter

data, we can take our calculations for the molar extinction ratio, and break it up among the scattering and absorption components. The molar absorption and scattering coefficients for the LSPR are shown in Table 1. The same is shown for the SSPR contributed by the axial modes in Table 2. Some observations:

1. The absorption coefficient for the 10x45 nm GNRs is seven times less than the 25x86 nm GNRs even though the absorption for the 10x45 nm nanorods is 90% of the extinction coefficient whereas its only 65% for the 25x86 nm. This reduction is offset by the fact that the 10x45 nm have ten times the concentration at OD 1 than the 25x86 nm GNRs, combined with the fact that the 10x45 nm will circulate much, much longer in-vivo due to their smaller size.
2. The SSPR from the axial mode of the GNRs is still five orders of magnitude greater than quantum dots in the visible.
3. The LSPR for the 10 nm GNRs absorb over 70% of incident power at OD 1 in only 1 cm of path length.
4. The SSPR for the GNRs absorb 15-20% of incident power at OD 1 in only 1 cm of path length.

In order to demonstrate this effect, we used a small, 1 cm path length cuvette of 10x41 nanorods at OD 1 in water. Since the specific heat of water is 4 joules/cm³ K, this means that with a 1 W/cm² laser at 808 nm, the water should heat at approximately 1 degree every second.

The following equations calculate this heat absorption:

$$A = \log\left(\frac{P_0}{P}\right) \quad (1)$$

Where A is the absorption, P₀ is the power before the GNRs and P is the power measured that has been transmitted through the GNRs.

$$A = \epsilon dC \quad (2)$$

Where ϵ is the molar extinction coefficient (M⁻¹cm⁻¹), d is the thickness of the sample (cm), and C is the concentration in moles/L.

Referring to Table 1, our 30-10-808 has an $\epsilon = 1.02 \times 10^9$ M⁻¹cm⁻¹, our cuvette is 1 cm thick, and the concentration C = 5.9x10¹¹ gnrs/ml, or 1x10⁻⁷ moles/L. Therefore, A = 0.578, or 73% of the power is absorbed in the GNRs in 1 cm.

Possible Applications

The selective ability to use specific directional and wavelengths in laser to initiate localized heating

has far reaching applications in the nanotechnology world. These applications could involve:

1. Heat generated chemical reactions at the nanoscale.
2. Wavelength selected heat generated reactions at the nanoscale.
3. Heating by confocal microscopy delineating micron selected areas.
4. Nano-welding in semiconductor applications.
5. Improved solar cell collection.
6. Coating for an improved solar water heater.

**Ntracker™ Photothermal Conversion
Efficiency in Water**

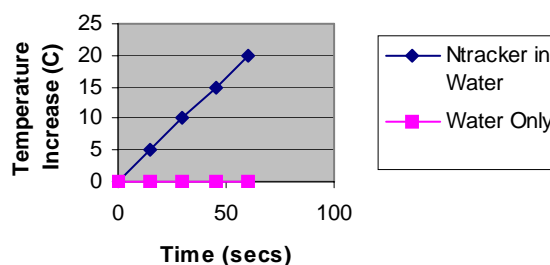


Figure 3 Thermal conversion efficiency in water at standard OD 1 concentration.

References

1. Lee, K.-S.; El-Sayed, M. A. Dependence of the Enhanced Optical Scattering Efficiency Relative to That of Absorption for Gold Metal Nanorods on Aspect Ratio, Size, End-Cap Shape, and Medium Refractive Index. *J. Phys. Chem. B* **2005**, *109*, 20331–20338.
2. Jain, P. K.; Lee, K. S.; El-Sayed, I. H.; El-Sayed, M. A. Calculated Absorption and Scattering Properties of Gold Nanoparticles of Different Size, Shape, and Composition: Applications in Biological Imaging and Biomedicine. *J. Phys. Chem. B* **2006**, *110*, 7238–7248.
3. Chen, W. R.; Adams, R. L.; Carubelli, R.; Nordquist, R. E. Laser-Photosensitizer Assisted Immunotherapy: A Novel Modality for Cancer Treatment. *Cancer Lett.* **1997**, *115*, 25–30.
4. Gorelikov, I.; Field, L. M.; Kumacheva, E. Hybrid Microgels Photoresponsive in the Near-Infrared Spectral Range. *J. Am. Chem. Soc.* **2004**, *126*, 15938–15939.
5. Karg, M.; Pastoriza-Santos, I.; Pérez-Juste, J.; Hellweg, T.; Liz-Marzán, L. M. Nanorod-Coated PNIPAM Microgels: Thermoresponsive Optical Properties. *Small* **2007**, *3*, 1222–1229.
6. Pérez-Juste, J.; Rodríguez-González, B.; Mulvaney, P.; Liz-Marzán, L. M. Optical Control and Patterning of Gold-Nanorod-Poly(vinyl alcohol) Nanocomposite Films. *Adv. Funct. Mater.* **2005**, *15*, 1065–1071.
7. Murphy, C. J.; Orendorff, C. J. Alignment of Gold Nanorods in Polymer Composites and on Polymer Surfaces. *Adv. Mater.* **2005**, *17*, 2173–2177.
8. Chon, J. W. M.; Bullen, C.; Zijlstra, P.; Gu, M. Spectral Encoding on Gold Nanorods Doped in a Silica Sol-Gel Matrix and Its Application to High-Density Optical Data Storage. *Adv. Funct. Mater.* **2007**, *17*, 875–880.
9. Berry, V.; Gole, A.; Kundu, S.; Murphy, C. J.; Saraf, R. F. Deposition of CTAB-Terminated Nanorods on Bacteria to Form Highly Conducting Hybrid Systems. *J. Am. Chem. Soc.* **2005**, *127*, 17600–17601.
10. Katz, E.; Willner, I. Integrated Nanoparticle-Biomolecule Hybrid Systems: Synthesis, Properties, and Applications. *Angew. Chem., Int. Ed.* **2004**, *43*, 6042–6108.
11. Sudeep, P. K.; Joseph, S. T. S.; Thomas, K. G. Selective Detection of Cysteine and Glutathione Using Gold Nanorods. *J. Am. Chem. Soc.* **2005**, *127*, 6516–6517.
12. Wang, H. F.; Huff, T. B.; Zweifel, D. A.; He, W.; Low, P. S.; Wei, A.; Cheng, J.-X. *In Vitro* and *In Vivo* Two-Photon Luminescence Imaging of Single Gold Nanorods. *Proc. Natl. Acad. Sci. U.S.A.* **2005**, *102*, 15752–15756.
13. Durr, N. J.; Larson, T.; Smith, D. K.; Korgel, B. A.; Sokolov, K.; Ben-Yakar, A. Two-Photon Luminescence Imaging of Cancer Cells Using Molecularly Targeted Gold Nanorods. *Nano Lett.* **2007**, *7*, 941–945.
14. Huang, X. H.; El-Sayed, I. H.; Qian, W.; El-Sayed, M. A. Cancer Cells Assemble and Align Gold Nanorods Conjugated to Antibodies to Produce Highly Enhanced, Sharp, and Polarized Surface Raman Spectra: A Potential Cancer Diagnostic Marker. *Nano Lett.* **2007**, *7*, 1591–1597.
15. Huang, X. H.; El-Sayed, I. H.; Qian, W.; El-Sayed, M. A. Cancer Cell Imaging and Photothermal Therapy in the Near-Infrared Region by Using Gold Nanorods. *J. Am. Chem. Soc.* **2006**, *128*, 2115–2120.

16. Chen, C.-C.; Lin, Y.-P.; Wang, C.-W.; Tzeng, H.-C.; Wu, C.-H.; Chen, Y.-C.; Chen, C.-P.; Chen, L.-C.; Wu, Y.-C. DNA-Gold Nanorod Conjugates for Remote Control of Localized Gene Expression by Near Infrared Irradiation. *J. Am. Chem. Soc.* **2006**, *128*, 3709–3715.
17. Weissleder, R. A Clearer Vision for *In Vivo* Imaging. *Nat. Biotechnol.* **2001**, *19*, 316–317.
18. Hirsch, L. R.; Stafford, R. J.; Bankson, J. A.; Sershen, S. R.; Rivera, B.; Price, R. E.; Hazle, J. D.; Halas, N. J.; West, J. L. Nanoshell-Mediated Near-Infrared Thermal Therapy of Tumors under Magnetic Resonance Guidance. *Proc. Natl. Acad. Sci. U.S.A.* **2003**, *100*, 13549–13554.
19. Loo, C.; Lowery, A.; Halas, N.; West, J.; Drezek, R. Immunotargeted Nanoshells for Integrated Cancer Imaging and Therapy. *Nano Lett.* **2005**, *5*, 709–711.
20. Chen, J. Y.; Saeki, F.; Wiley, B. J.; Cang, H.; Cobb, M. J.; Li, Z.-Y.; Au, L.; Zhang, H.; Kimmey, M. B.; Li, X. D.; Xia, Y. N. Gold Nanocages: Bioconjugation and Their Potential Use as Optical Imaging Contrast Agents. *Nano Lett.* **2005**, *5*, 473–477.
21. Weihai Ni, Xiaoshan Kou, Zhi Yang, and Jianfang Wang, Tailoring Longitudinal Surface Plasmon Wavelengths, Scattering and Absorption Cross Sections of Gold Nanorods, *ACS Nano*, Vol. 2 No. 4, 677-686, **2008**.

Table 1 Molar Absorption and Scattering for GNR LSPR

Part # Nanorod (Axial Diam/Peak LSPR)	Axial Diameter (nm)	Longitudinal Size (nm)	Peak LSPR Wavelength (nm)	OD LSPR (AU)	NPS/ml	Wt. conc (mg/ml)	Molarity (pM)	LSPR Molar Ext. (M- 1cm-1)	LSPR Molar Absorption (M-1cm-1)	LSPR Molar Scattering (M-1cm-1)	% Abs of Incident Power through 1 cm at OD1
30-10-850	10	45	850	1.0	5.2E+11	35.7	874	1.14E+09	1.03E+09	1.14E+08	73.1%
30-10-808	10	41	808	1.0	5.9E+11	36.1	979	1.02E+09	9.19E+08	1.02E+08	73.1%
30-10-780	10	38	780	1.0	6.1E+11	34.9	1020	9.81E+08	8.83E+08	9.81E+07	73.1%
30-10-750	10	35	750	1.0	6.4E+11	33.4	1064	9.40E+08	8.46E+08	9.40E+07	73.1%
30-10-700	10	29	700	1.0	6.7E+11	29.7	1112	8.99E+08	8.09E+08	8.99E+07	73.1%
30-25-750	25	86	750	1.0	5.2E+10	42.9	87	1.14E+10	7.44E+09	4.00E+09	42.1%
30-25-700	25	73	700	1.0	1.3E+11	91.1	218	4.58E+09	2.97E+09	1.60E+09	42.1%
30-25-650	25	60	650	1.0	2.6E+11	149.8	437	2.29E+09	1.49E+09	8.01E+08	42.1%
30-25-600	25	47	600	0.9	5.2E+11	235.1	874	1.03E+09	6.69E+08	3.60E+08	36.4%
30-25-550	25	34	550	0.8	5.2E+11	170.5	874	9.15E+08	5.95E+08	3.20E+08	31.6%

Table 2 Molar Absorption and Scattering for GNR SSPR

Part # Nanorod (Axial Diam/Peak LSPR)	Axial Diameter (nm)	Longitudinal Size (nm)	Peak SSRP Wavelength (nm)	OD SSPR (AU)	NPS/ml	Wt. conc (mg/ml)	Molarity (pM)	SSPR Molar Ext. (M- 1cm-1)	SSPR Molar Absorption (M-1cm-1)	SSPR Molar Scattering (M-1cm-1)	% Abs of Incident Power through 1 cm at OD1
30-10-850	10	45	512	0.25	5.2E+11	35.7	874	2.86E+08	2.57E+08	2.86E+07	16.4%
30-10-808	10	41	512	0.25	5.9E+11	36.1	979	2.55E+08	2.30E+08	2.55E+07	16.4%
30-10-780	10	38	512	0.25	6.1E+11	34.9	1020	2.45E+08	2.21E+08	2.45E+07	16.4%
30-10-750	10	35	512	0.25	6.4E+11	33.4	1064	2.35E+08	2.11E+08	2.35E+07	16.4%
30-10-700	10	29	512	0.25	6.7E+11	29.7	1112	2.25E+08	2.02E+08	2.25E+07	16.4%
30-25-750	25	86	530	0.50	5.2E+10	42.9	87	5.72E+09	3.72E+09	2.00E+09	20.5%
30-25-700	25	73	530	0.50	1.3E+11	91.1	218	2.29E+09	1.49E+09	8.01E+08	20.5%
30-25-650	25	60	530	0.50	2.6E+11	149.8	437	1.14E+09	7.44E+08	4.00E+08	20.5%
30-25-600	25	47	530	0.50	5.2E+11	235.1	874	5.72E+08	3.72E+08	2.00E+08	20.5%
30-25-550	25	34	530	0.50	5.2E+11	170.5	874	5.72E+08	3.72E+08	2.00E+08	20.5%